Scientia Iranica D (2018) 25(3), 1608–1615

Sharif University of Technology
Scientia Iranica
Transactions D: Computer Science & Engineering and Electrical Engineering
http://scientiairanica.sharif.edu

Research Note

The effect of uniaxial and torsional strains on the density of states of single walled carbon nanotubes

M. Pakkhesal and S.E. Hosseini*

Department of Electrical Engineering, Faculty of Engineering, Ferdowsi University of Mashhad, Mashhad, Iran.

Received 12 June 2015; received in revised form 30 August 2016; accepted 3 October 2016

KEYWORDS
Tight binding;
Carbon nanotubes;
Density of states;
Electronic band structure;
Uniaxial strain;
Torsional strain.

Abstract. In this paper, we investigate the effect of uniaxial and torsional strains on the Density of States (DoS) of single walled Carbon nanotubes (SWCNTs). We employ the nearest neighbor and also the third nearest neighbor π-TB (Tight Binding) models for our investigation. It is shown that uniaxial and torsional strains in some cases of metallic SWCNTs not only open a band gap, but also effectively increase the DoS of SWCNT. It is also shown that the mentioned types of strain have different effects on the DoS of chiral SWCNTs; in some types, they increase the DoS at the band edges, while they decrease it at the band edges in other types.

1. Introduction

It has past more than two decades from the exploration of Carbon nanotubes (CNTs) now [1]; however, the technology of fabrication has been considered the most important restriction on the development of CNTs as applicable materials for the fabrication of the nano-electronic circuits. Nonetheless, studies have continued to investigate the physical and electronic properties of carbon nanotubes [2-5]. It is well known that strain can significantly modify CNT electronic properties, such as band-gap and density of states. This alters electronic applications of CNTs. One of the most important electronic properties of SWCNTs is their Density of States (DoS), especially near the band gap. A high DoS at a specific energy level means that there are many states available for occupation. A DoS of zero means that no states can be occupied at that energy level. The product of the density of states and the probability distribution function are the number of occupied states per unit volume at a given energy for a system in thermal equilibrium. This value is widely used to investigate various physical properties of matter. Therefore, the variation of the DoS in a semiconductor can seriously affect its physical properties, e.g. the electronic transport and optoelectronic properties. In this paper, we are to calculate precisely the variations of the DoS of SWCNTs due to uniaxial and torsional strains using a third neighbor tight-binding approach. For the first time, Mintmire and White [6] investigated DoS of SWCNTs using π-TB model. The advantage of π-TB model over the others for the calculation of the electronic band structure is the simplicity of the method, medium to good accuracy, and the analytical formula for the energy in a wide variety of cases, enabling us to perform some analyses on the energy and its dependencies. For example, Yang et al. [7] uses this model to investigate analytically the band gap variation of SWCNTs due to uniaxial and torsional strains. However, it is not always possible to acquire an analytical formula. In this paper, we investigate the effect of uniaxial and torsional strains on

---

*. *Corresponding author.*
E-mail addresses: pakkhesal_mehdi@yahoo.com (M. Pakkhesal); ehosseini@um.ac.ir (S.E. Hosseini)

doi: 10.24200/sci.2017.4366

the density of states of SWCNTs using semi-analytical formulae. Our work not only addresses armchair and zig-zag types, but also presents an approach for chiral nanotubes, and the effect of torsional strain is also investigated. Nonetheless, we have taken into account the effect of the second and third neighboring atoms (3-NN-TB) in addition to the nearest ones (1-NN-TB) for our tight-binding calculations. Most of other studies are concentrated on band gap variations [8-10] and electrical conductivity [11,12] due to uniaxial and torsional stresses. In addition, some other investigations focused on DoS without regarding mechanical deformations. This paper is organized as follows. In Section 2, π-TB model (either the nearest neighbor or the third nearest neighbor model) and the method of DoS calculation are introduced. Section 3 deals with the application of the method to some SWCNTs with different chiral vectors, observation, and comparison of the results. At last, in Section 4, we briefly add up the results to conclude the paper.

2. Method

Theoretically, it is known that a single walled carbon nanotube is made by rolling up of a graphene sheet into a cylinder so that the beginning and end of the lattice vector, so-called chiral vector **C**, can join. One can write that:

$$\vec{\mathbf{C}} = n_1\hat{\mathbf{a}}_1 + n_2\hat{\mathbf{a}}_2, \tag{1}$$

where $\vec{\mathbf{C}}$, $\hat{\mathbf{a}}_1$, and $\hat{\mathbf{a}}_2$ are shown in Figure 1. Additionally, one can define $\vec{\mathbf{T}}$ as the vector of translational symmetry as follows:

$$\vec{\mathbf{T}} = \frac{-(n_1+2n_2)\hat{\mathbf{a}}_1 + (2n_1+n_2)\hat{\mathbf{a}}_2}{GCD(n_1+2n_2, 2n_1+n_2)}. \tag{2}$$

As is known, under mechanical strain, the lattice is deformed, meaning that the distances from an atom to its neighboring atoms vary. Therefore, the first step is to calculate the new distances. To do this, we first need to calculate unit vectors along circumference $\hat{\mathbf{c}}$ and along the axis of nanotube $\hat{\mathbf{t}}$ perpendicular to $\hat{\mathbf{c}}$. From the continuum mechanics, we know that:

$$r_{it} \to r_{it}(1+\sigma_t), \tag{3a}$$

$$r_{ic} \to r_{ic} + r_{it}\tan(\alpha) \quad (i=1,2,3), \tag{3b}$$

where α is the angle of shear and σ_t is the percent of tensile. Subscripts t and c denote the parts of $\mathbf{r}_\mathbf{i}$, (shown in Figure 1) which are along the axis of the nanotube and in azimuthal direction (around the circumference of the nanotube), respectively. From Eqs. (1) and (2), one can write that:

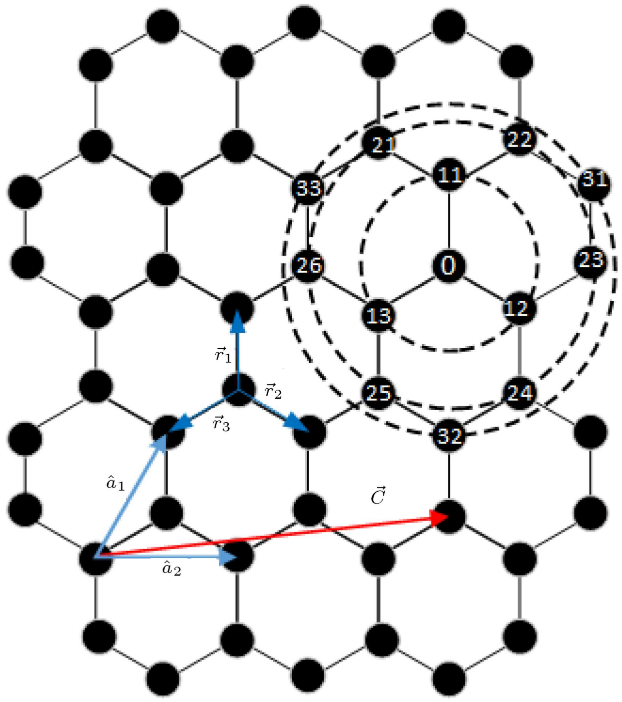

Figure 1. Graphene sheet with lattice vector **C** and unit vectors $\mathbf{a}_1$ and $\mathbf{a}_2$. The three neighborhoods of atom 0 are also shown, i.e. most inner circles are the nearest neighbors, the mid circle shows the second neighboring atoms, and most outer circles pass through the third neighboring atoms.

$$\hat{\mathbf{c}} = \frac{n_1\hat{\mathbf{a}}_1 + n_2\hat{\mathbf{a}}_2}{ac_h}, \tag{4a}$$

$$\hat{\mathbf{t}} = \frac{-(n_1+2n_2)\hat{\mathbf{a}}_1 + (2n_1+n_2)\hat{\mathbf{a}}_2}{\sqrt{3}ac_h}, \tag{4b}$$

where $\hat{\mathbf{c}}$ and $\hat{\mathbf{t}}$ are the azimuthal and translational unit vectors, $a = |\hat{\mathbf{a}}_1| = |\hat{\mathbf{a}}_2|$ and $c_h = \sqrt{n_1^2 + n_2^2 + n_1 n_2}$. In the absence of strain, by solving Eqs. (4a) and (4b) for $\hat{\mathbf{a}}_1$ and $\hat{\mathbf{a}}_2$, we find that:

$$\hat{\mathbf{a}}_1 = \frac{\sqrt{3}}{2}\frac{a}{c_h}\left(\frac{2n_1+n_2}{\sqrt{3}}\hat{\mathbf{c}} - n_2\hat{\mathbf{t}}\right), \tag{5a}$$

$$\hat{\mathbf{a}}_2 = \frac{\sqrt{3}}{2}\frac{a}{c_h}\left(\frac{n_1+2n_2}{\sqrt{3}}\hat{\mathbf{c}} + n_1\hat{\mathbf{t}}\right). \tag{5b}$$

Therefore, according to Figure 1, we have:

$$\vec{\mathbf{r}}_1 = \frac{2\vec{\mathbf{a}}_1 - \vec{\mathbf{a}}_2}{3} = \frac{1}{2\sqrt{3}}\frac{a}{c_h}\left[\sqrt{3}n_1\hat{\mathbf{c}} - (n_1+2n_2)\hat{\mathbf{t}}\right], \tag{6a}$$

$$\vec{\mathbf{r}}_2 = \frac{2\vec{\mathbf{a}}_2 - \vec{\mathbf{a}}_1}{3} = \frac{1}{2\sqrt{3}}\frac{a}{c_h}\left[\sqrt{3}n_2\hat{\mathbf{c}} + (2n_1+n_2)\hat{\mathbf{t}}\right], \tag{6b}$$

$$\vec{\mathbf{r}}_3 = -\left(\vec{\mathbf{r}}_1 + \vec{\mathbf{r}}_2\right) = -\frac{1}{2\sqrt{3}}\frac{a}{c_h}\left[\sqrt{3}(n_1+n_2)\hat{\mathbf{c}} + (n_1-n_2)\hat{\mathbf{t}}\right]. \tag{6c}$$

Then, we define $r_0 = |\vec{\mathbf{r}}_i|$ $(i = 1, 2, 3)$ in the absence of strain. Next, we use Relations (3a) and (3b) to calculate $\vec{\mathbf{r}}_1$, $\vec{\mathbf{r}}_2$, and $\vec{\mathbf{r}}_3$ in the presence of strain, which are:

$$\vec{\mathbf{r}}_1 = \frac{1}{2\sqrt{3}}\frac{a}{c_h}\left\{\left[\sqrt{3}n_1 - (n_1+2n_2)\tan(\alpha)\right]\hat{\mathbf{c}} - (n_1+2n_2)(1+\sigma_t)\hat{\mathbf{t}}\right\}, \tag{7a}$$

$$\vec{\mathbf{r}}_2 = \frac{1}{2\sqrt{3}}\frac{a}{c_h}\left\{\left[\sqrt{3}n_2 + (2n_1+n_2)\tan(\alpha)\right]\hat{\mathbf{c}} + (2n_1+n_2)(1+\sigma_t)\hat{\mathbf{t}}\right\}, \tag{7b}$$

$$\vec{\mathbf{r}}_3 = -\frac{1}{2\sqrt{3}}\frac{a}{c_h}\left\{\left[\sqrt{3}(n_1+n_2)+(n_1-n_2)\tan(\alpha)\right]\hat{\mathbf{c}} + (n_1-n_2)(1+\sigma_t)\hat{\mathbf{t}}\right\}. \tag{7c}$$

They enable us to define $r_i = |\vec{\mathbf{r}}_i|$ $(i = 1, 2, 3)$ in the presence of strain. Also:

$$\hat{\mathbf{a}}_1 = \frac{\sqrt{3}}{2}\frac{a}{c_h}\left\{\left[\frac{2n_1+n_2}{\sqrt{3}} - n_2\tan(\alpha)\right]\hat{\mathbf{c}} - n_2(1+\sigma_t)\hat{\mathbf{t}}\right\}, \tag{8a}$$

$$\hat{\mathbf{a}}_2 = \frac{\sqrt{3}}{2}\frac{a}{c_h}\left\{\left[\frac{n_1+2n_2}{\sqrt{3}} + n_1\tan(\alpha)\right]\hat{\mathbf{c}} + n_1(1+\sigma_t)\hat{\mathbf{t}}\right\}. \tag{8b}$$

In this step, we can calculate the energy. The nearest neighbor π-TB energy is worked out as shown in Box I, [7], where $\gamma_{0i} = \gamma_0(\frac{r_0}{r_{0i}})^2$. γ_0 and r_0 are the hopping parameter and bond length in an unstrained lattice. In Eq. (9), we have:

$$\vec{\mathbf{k}}.\hat{a}_1 = \frac{\sqrt{3}}{2}\frac{a}{c_h}\left\{\left[\frac{2n_1+n_2}{\sqrt{3}} - n_2\tan(\alpha)\right]k_c - n_2(1+\sigma_t)k_t\right\}, \tag{10a}$$

$$\vec{\mathbf{k}}.\hat{a}_2 = \frac{\sqrt{3}}{2}\frac{a}{c_h}\left\{\left[\frac{n_1+2n_2}{\sqrt{3}} + n_1\tan(\alpha)\right]k_c + n_1(1+\sigma_t)k_t\right\}, \tag{10b}$$

where k_t is the part of $\mathbf{k}$ along the axis of the nanotube and k_c is acquired using Born-von-Karman boundary condition which is:

$$\vec{\mathbf{k}}.\vec{\mathbf{C}} = 2\pi q, \tag{11a}$$

or:

$$k_c c_h a = 2\pi q, \tag{11b}$$

where q is the sub-band index. The next step is to calculate the density of states using the well-known equation [6]:

$$n(E) = \frac{2}{l}\sum_q \int \delta(k-k_q)\left|\frac{\partial E}{\partial k}\right| dk, \tag{12}$$

where $n(E)$ is $\frac{\partial N(E)}{\partial E}$, $N(E)$ is the total number of states per unit cell below a given energy E, and l is the length of one-dimensional Brillouin zone that is equal to the total area of the first Brillouin zone $(\frac{8\pi^2}{a^2\sqrt{3}})$ divided by the interline spacing (according to Eq. (11b), it is: $\Delta k_c = \frac{2\pi}{a c_h}$) which yields:

$$l = \frac{4\pi}{\sqrt{3}}\frac{c_h}{a}. \tag{13}$$

Next, note that each line in the vicinity of the point located at $\mathbf{k_F}$ will have two points at any given energy; in addition to these two points, two more equivalent points in the vicinity of the point located at $-\mathbf{k_F}$ will contribute to the DoS at this energy. We can write the DoS per carbon atom, $\rho(E)$, as:

$$\rho(E) = \frac{n(E)}{2} = \frac{4}{l}\sum_{\substack{\text{all } k\text{'s on all}\\ \text{subbands having}\\ \text{the energy } E}} \left|\frac{\partial E}{\partial k_{||}}\right|^{-1}. \tag{14}$$

$$E^{\pm}\left(\vec{\mathbf{k}}\right) = \sqrt{\gamma_{01}^2 + \gamma_{02}^2 + \gamma_{03}^2 + 2\gamma_{01}\gamma_{03}\cos\left(\vec{\mathbf{k}}.\hat{\mathbf{a}}_1\right) + 2\gamma_{02}\gamma_{03}\cos\left(\vec{\mathbf{k}}.\hat{\mathbf{a}}_2\right) + 2\gamma_{01}\gamma_{02}\cos\left[\vec{\mathbf{k}}.\left(\hat{\mathbf{a}}_2 - \hat{\mathbf{a}}_1\right)\right]}. \tag{9}$$

Box I

$$\frac{\partial E^{\pm}}{\partial k_t} = (1+\sigma_t)\frac{\sqrt{3}}{2}\frac{a}{c_h}\frac{n_2\gamma_{01}\gamma_{03}\sin\left(\vec{\mathbf{k}}.\hat{a}_1\right) - n_1\gamma_{02}\gamma_{03}\sin\left(\vec{\mathbf{k}}.\hat{a}_2\right) + (n_2-n_1)\gamma_{01}\gamma_{02}\sin\left[\vec{\mathbf{k}}.\left(\hat{\mathbf{a}}_2-\hat{\mathbf{a}}_1\right)\right]}{E^{\pm}\left(\vec{\mathbf{k}}\right)}. \tag{15}$$

Box II

In Eqs. (10a) and (10b), we have $k_{||} = k_t$; therefore, $\frac{\partial E}{\partial k_{||}} = \frac{\partial E}{\partial k_t}$. For the nearest neighbor TB, we have Eq. (15) as shown in Box II, where $\vec{\mathbf{k}}.\vec{\mathbf{a}}_1$ and $\vec{\mathbf{k}}.\hat{\mathbf{a}}_2$ should be obtained from Eqs. (10a) and (10b), respectively, and k_c is equal to $\frac{2\pi q}{c_h a}$ as mentioned before. With the second nearest neighbor atoms and the third nearest neighbor atoms (shown in Figure 1) included in TB calculations, in addition to the nearest ones, we can increase the degrees of the accuracy of the results [13] and catch up the following [14] (with minor mathematic manipulations and corrections):

$$E^{\pm}\left(\vec{\mathbf{k}}\right) = \frac{-(-2E_0+E_1 \pm \sqrt{(-2E_0+E_1)^2-4E_2E_3}}{2E_3}, \tag{16}$$

with:

$$E_0 = S_{AA}H_{AA} = \left[1+s_1 u\left(\vec{\mathbf{k}}\right)\right]\left[\varepsilon_{2p}+\gamma_1 u\left(\vec{\mathbf{k}}\right)\right], \tag{17a}$$

$$\begin{aligned} E_1 =& S_{AB}H^*_{AB} + S^*_{AB}H_{AB} = f_{s\gamma}\left(\vec{\mathbf{k}}\right) + s_2 g_\gamma\left(\vec{\mathbf{k}}\right) \\ &+ \gamma_2 g_s\left(\vec{\mathbf{k}}\right) + 2s_2\gamma_2 f\left(2\vec{\mathbf{k}}\right), \end{aligned} \tag{17b}$$

$$\begin{aligned} E_2 =& H^2_{AA} - H_{AB}H^*_{AB} = \left[\varepsilon_{2p}+\gamma_1 u\left(\vec{\mathbf{k}}\right)\right]^2 \\ &- f_{\gamma\gamma}\left(\vec{\mathbf{k}}\right) - \gamma_2 g_\gamma\left(\vec{\mathbf{k}}\right) - \gamma_2^2 f\left(2\vec{\mathbf{k}}\right), \end{aligned} \tag{17c}$$

$$\begin{aligned} E_3 =& S^2_{AA} - S_{AB}S^*_{AB} = \left[1+s_1 u\left(\vec{\mathbf{k}}\right)\right]^2 \\ &- f_{ss}\left(\vec{\mathbf{k}}\right) - s_2 g_s\left(\vec{\mathbf{k}}\right) - s_2^2 f\left(2\vec{\mathbf{k}}\right), \end{aligned} \tag{17d}$$

and:

$$\begin{aligned} u\left(\vec{\mathbf{k}}\right) =& 2\cos\left(\vec{\mathbf{k}}.\hat{\mathbf{a}}_1\right) + 2\cos\left(\vec{\mathbf{k}}.\hat{\mathbf{a}}_2\right) \\ &+ 2\cos\left[\vec{\mathbf{k}}.\left(\hat{\mathbf{a}}_2-\hat{\mathbf{a}}_1\right)\right], \end{aligned} \tag{18a}$$

$$f\left(\vec{\mathbf{k}}\right) = 3 + u\left(\vec{\mathbf{k}}\right), \tag{18b}$$

$$\begin{aligned} f_{s\gamma}(\vec{\mathbf{k}}) =& 2(s_{01}\gamma_{01} + s_{02}\gamma_{02} + s_{03}\gamma_{03}) \\ &+ 2\left(s_{01}\gamma_{03} + \gamma_{01}s_{03}\right)\cos\left(\vec{\mathbf{k}}.\hat{\mathbf{a}}_1\right) \\ &+ 2\left(s_{02}\gamma_{03} + \gamma_{02}s_{03}\right)\cos\left(\vec{\mathbf{k}}.\hat{\mathbf{a}}_2\right) \\ &+ 2\left(s_{01}\gamma_{02} + \gamma_{01}s_{02}\right)\cos\left[\vec{\mathbf{k}}.\left(\hat{\mathbf{a}}_2-\hat{\mathbf{a}}_1\right)\right], \end{aligned} \tag{18c}$$

$$\begin{aligned} f_{\gamma\gamma}(\vec{\mathbf{k}}) =& \gamma_{01}^2 + \gamma_{02}^2 + \gamma_{03}^2 + 2\gamma_{01}\gamma_{03}\cos\left(\vec{\mathbf{k}}.\hat{\mathbf{a}}_1\right) \\ &+ 2\gamma_{02}\gamma_{03}\cos\left(\vec{\mathbf{k}}.\hat{\mathbf{a}}_2\right) \\ &+ 2\gamma_{01}\gamma_{02}\cos\left[\vec{\mathbf{k}}.\left(\hat{\mathbf{a}}_2-\hat{\mathbf{a}}_1\right)\right], \end{aligned} \tag{18d}$$

$$\begin{aligned} f_{ss}(\vec{\mathbf{k}}) =& s_{01}^2 + s_{02}^2 + s_{03}^2 + 2s_{01}s_{03}\cos\left(\vec{\mathbf{k}}.\hat{\mathbf{a}}_1\right) \\ &+ 2s_{02}s_{03}\cos\left(\vec{\mathbf{k}}.\hat{\mathbf{a}}_2\right) \\ &+ 2s_{01}s_{02}\cos\left[\vec{\mathbf{k}}.\left(\hat{\mathbf{a}}_2-\hat{\mathbf{a}}_1\right)\right], \end{aligned} \tag{18e}$$

$$\begin{aligned} u_\gamma\left(\vec{\mathbf{k}}\right) =& 2\gamma_{02}\cos\left(\vec{\mathbf{k}}.\hat{\mathbf{a}}_1\right) + 2\gamma_{01}\cos\left(\vec{\mathbf{k}}.\hat{\mathbf{a}}_2\right) \\ &+ 2\gamma_{03}\cos\left[\vec{\mathbf{k}}.\left(\hat{\mathbf{a}}_2-\hat{\mathbf{a}}_1\right)\right], \end{aligned} \tag{18f}$$

$$\begin{aligned} u_s\left(\vec{\mathbf{k}}\right) =& 2s_{02}\cos\left(\vec{\mathbf{k}}.\hat{\mathbf{a}}_1\right) + 2s_{01}\cos\left(\vec{\mathbf{k}}.\hat{\mathbf{a}}_2\right) \\ &+ 2s_{03}\cos\left[\vec{\mathbf{k}}.\left(\hat{\mathbf{a}}_2-\hat{\mathbf{a}}_1\right)\right], \end{aligned} \tag{18g}$$

$$g_\gamma\left(\vec{\mathbf{k}}\right) = 2u_\gamma\left(\vec{\mathbf{k}}\right) + u_\gamma\left(k_1-2k_2, 2k_1-k_2\right), \tag{18h}$$

$$g_s\left(\vec{\mathbf{k}}\right) = 2u_s\left(\vec{\mathbf{k}}\right) + u_s\left(k_1-2k_2, 2k_1-k_2\right). \tag{18i}$$

The values of γ_0, γ_1, γ_2, s_0, s_1, s_2, and ε_{2p} are shown in Table 1. Using Eqs. (10a) and (10b) in Eqs. (18a) to (18i), Eqs. (17a) to (17d) in Eq. (16), taking derivative with respect to k_t, and then using Eq. (14), we can work out DoS with the third neighbor tight-binding model.

Table 1. 3-NN tight-binding parameters and their values. The values are obtained by fitting to ab initio energies for k, yielding optical transitions with energy < 4 eV [13].

Parameter	ε_{2p}	γ_0	γ_1	λ_2	s_0	s_1	s_2
Value	−2.03	−2.79	−0.68	−0.30	0.30	0.046	0.039

3. Results and discussion

Illustrated in Figure 2 are the DoS's of SWCNT for a number of chiral vectors under 0, 1, 2, and 3 percents of uniaxial strain calculated by the nearest neighbor tight-binding model (1-NN-TB model). For zero percent of strain, our model perfectly matches that of [6]. From the band gap point of view and in the case uniaxial strain, the band gap change is maximum for the zig-zag nantubes and minimum for armchair nanotubes. In the case of chiral nanotubes, for uniaxial strain, $|\frac{dE_g}{d\sigma}|$ increases with increasing strain. The sign of the mentioned quantity follows $(n-m)$ mod 3 rule. The mentioned results agree with those of [7,8].

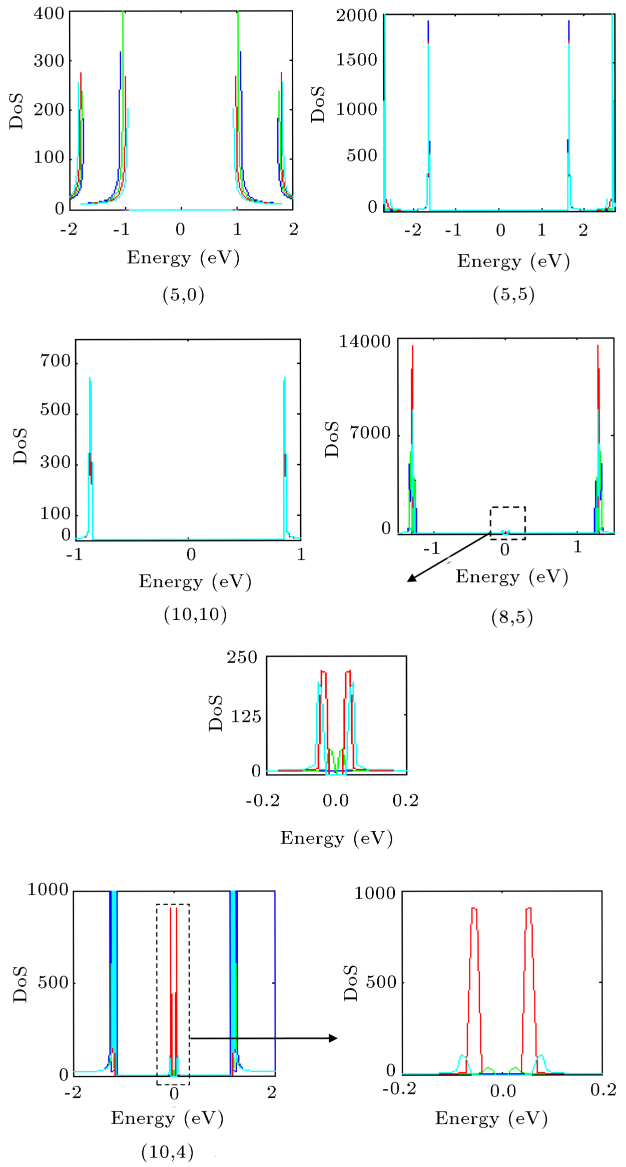

(5,0) (5,5)

(10,10) (8,5)

(10,4)

Figure 2. Density of States (DoS) per energy per carbon atom calculated using 1-NN-TB for a number of chiral vectors for zero (blue), one (green), two (red), and three (cyan) percent of uniaxial strain. The points of discontinuities happened due to the value of infinity due to our calculating software.

As can be seen in Figure 2, for a number of chiral vectors, uniaxial strain causes a moderate grow in DoS at the band edges, while it causes a moderate reduction in DoS for the other ones at the band edges. In this figure, the points of discontinuities are the van Hove singularities [15,16] where the DoS goes to infinity. For example, for (5,0) chiral vector, uniaxial strain causes a reduction in DoS as well as the value of band gap, while for (10,0) chiral vector, it causes an increase in both DoS and band gap.

As can be seen in this figure, for armchair tubes such as (5,5), uniaxial strain causes no serious change in both DoS and band gap. For non-armchair metallic (or semi metallic) tubes, it makes a band gap which increases with the increase of strain as well as its DoS as shown for (8,5) and (10,4) chiral vectors.

DoS and band gap are the same as illustrated in Figure 3, except that they are plotted regarding the second and third neighbors, in addition to the nearest ones (3-NN-TB model). As can be seen, there is no such symmetry around the mid-gap (zero point at the energy axis) as for Figure 2. This is the result of using 3-NN-TB model. As mentioned before, this model is shown to be more accurate and has better coincidence with ab-initio results. It is also observed that there are some variations of the DoS and band gap values.

Next, we apply our formulae to investigate the effect of torsional strain. Figure 4 illustrates the calculated DoS using 1-NN-TB model in the presence of torsional strain. The band gap change is approximately $3\gamma_0$ for the armchair nanotubes and is small for zig-zag nanotubes. In the case of chiral nanotubes, the torsional strain causes the band gap to decrease with the increasing degrees of shear. The sign of the mentioned quantity $(|\frac{dE_g}{d(\text{shear})}|)$ follows $(n-m)$ mod 3 rule, which again agrees with those of [7].

As can be seen in Figures 4 and 5 (which is the same in Figure 4 except that it is calculated using 3-NN-TB model), torsional strain has dramatic effect on

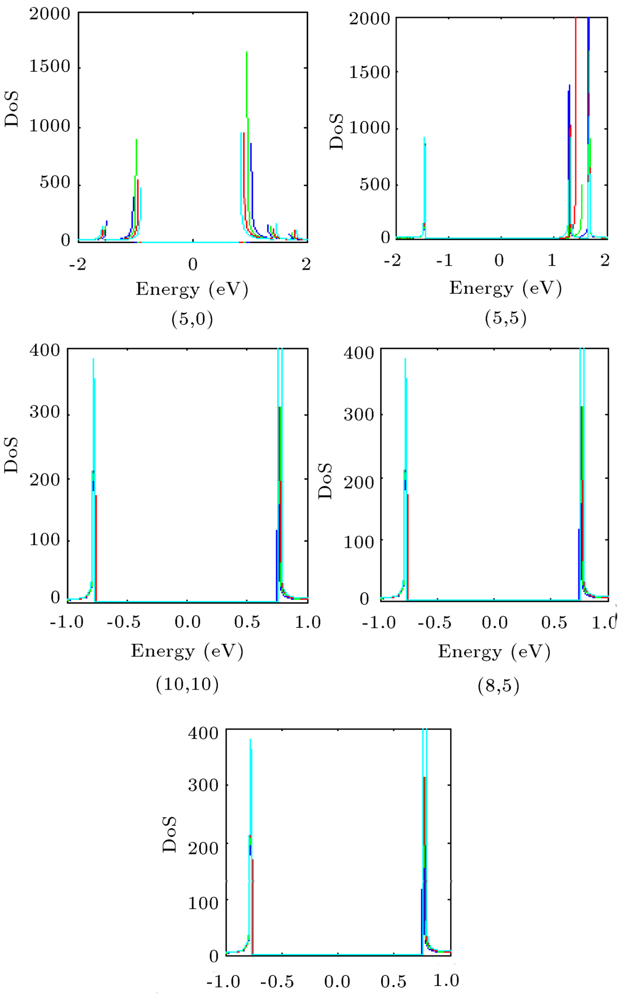

(5,0) (5,5)

(10,10) (8,5)

(10,4)

Figure 3. Density of States (DoS) per energy per carbon atom calculated using 3-NN-TB for a number of chiral vectors for zero (blue), one (green), two (red), and three (cyan) percents of uniaxial strain.

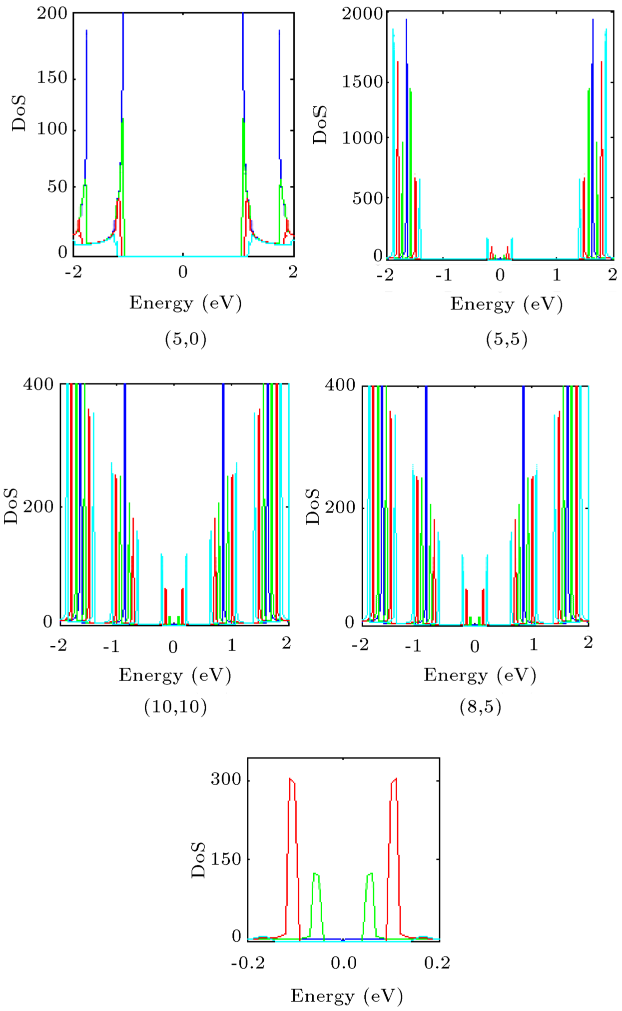

(5,0) (5,5)

(10,10) (8,5)

(10,4)

Figure 4. Density of States (DoS) per energy per carbon calculated using 1-NN-TB for a number of chiral vectors for zero (blue), one (green), two (red), and three (cyan) degrees of shear.

both band gap and density of states of armchair tubes. It causes the armchair tube to open a band gap, which increases with increasing strain. It also makes these kinds of tubes to increase the DoS with shear.

As is illustrated, torsional strain also opens a gap and increases the DoS in metallic (semi-metallic) chiral tubes such as (8,5) and (10,4). It is again worth mentioning that the discontinuities are equal to very large values of DoS whose software shows them as infinity (therefore, cannot be plotted accurately), and they are the well-known van Hove singularities.

4. Conclusion

In this paper, we investigated the effect of two types of strains, namely uniaxial and torsional strains on the DoS of SWCNTs. We used the nearest neighbor and the third nearest neighbor π-tight-binding models to calculate DoS. A semi-analytical approach was used for the computation of the strain effects. It was observed that these strains open band gaps in some cases, e.g. metallic CNTs, even for the armchair nanotubes. Our calculations showed that these two types of strain have dramatic effects on the DoS and band gap of SWCNTs. Moreover, accurate modeling of electronic properties requires considering the three atomic neighbors. Therefore, using the results of this paper helps to not only precisely predict the DoS variations, but also to more accurately make estimations concerning the electronic transport and the optoelectronic properties of SWCNTs. In some cases, they cause them to increase both of the band gap and DoS, and vice versa in some other cases.

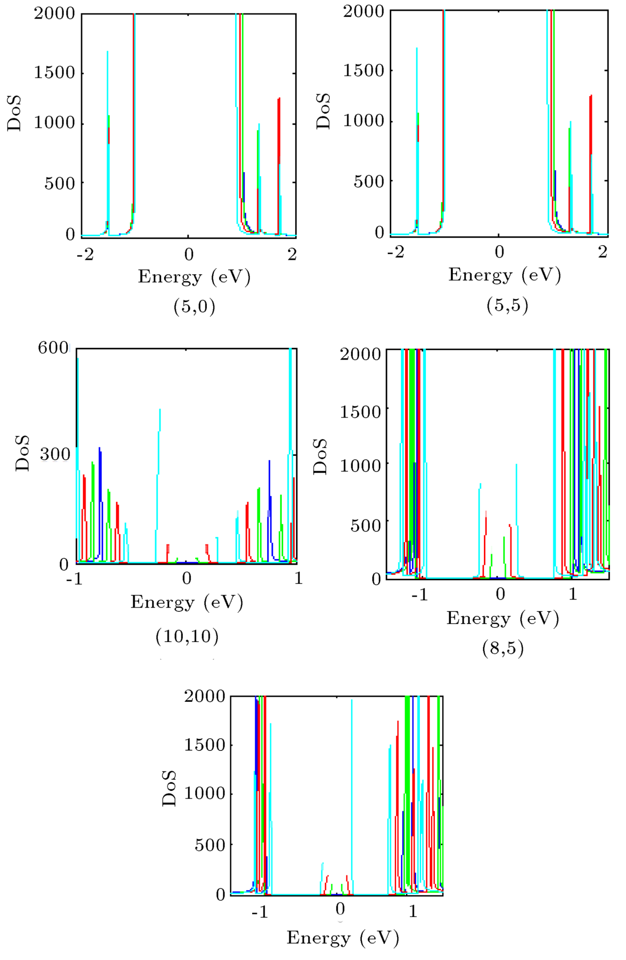

(5,0)

(5,5)

(10,10)

(8,5)

(10,4)

Figure 5. Density of States (DoS) per energy per carbon atom calculated using 3-NN-TB for a number of chiral vectors for zero (blue), one (green), two (red), and three (cyan) degrees of shear.

References

1. Iijima, S. "Helical microtubules of graphitic carbon", *Nature* (London), **354**, pp. 56-58 (1991).

2. Ahmadpour, M.T., Hashemifar, S.J., and Rostamnejadi, A. "Size effects on the structural, electronic, and optical properties of (5,0) finite-length carbon nanotube: An ab-initio electronic structure study", *J. App. Phys.*, **120**(1), p. 014303 (2016).

3. Hayashi, D., Ueda, T., Nakai, Y., Kyakuno, H., Miyata, Y., Yamamoto, T., Saito, T., Hata, K., and Maniwa, Y. "Thermoelectric properties of single-wall carbon nanotube films: Effects of diameter and wet environment", *App. Phys. Express*, **9**(2), pp. 0251021-0251024 (2016).

4. De Nicola, F., Salvato, M., Cirillo, C., Crivellarie, M., Boscardin, M., Scarselli, M., Nanni, F., Cacciotti, I., De Crescenzi, M., and Castrucci, P. "Record efficiency of air-stable multi-walled carbon nanotube/silicon solar cells", *Carbon*, **101**, pp. 226-234 (2016).

5. Liu, F., Nakajima, Y., and Wakabayashi, K. " Numerical study of carbon nanotubes under circularly polarized irradiation", *App. Phys. Express*, **9**(8), pp. 0851011-0851014 (2016).

6. Mintmire, J.W. and White, C.T. "Universal density of states for carbon nanotubes", *Phys. Rev. Lett.*, **81**(12), pp. 2506-2509 (1998).

7. Yang, L., Anantram, M.P., Han, J., and Lu, J.P. "Band-gap change of carbon nanotubes: Effect of small uniaxial and torsional strain", *Phys. Rev. B*, **60**(19), pp. 13874-13877 (1999).

8. Heyd, R., Charlier, A., and McRae, E. "Uniaxial-stress effects on the electronic properties of carbon nanotubes", *Phys. Rev. B*, **55**(11), pp. 6820-6824 (1997).

9. Li, E.Y. "Band gap engineering of carbon nanotubes via regular addition patterns of covalent functional groups", *Carbon*, **100**, pp. 187-195 (2016).

10. Qiu, M., Xie, Y., Gao, X., Li, J., Deng, Y., Guan, D., Maa, L., and Yuan, C. "Band gap opening and semiconductor-metal phase transition in (n, n) single-walled carbon nanotubes with distinctive boron-nitrogen line defect", *Phys. Chem. Chem. Phys.*, **18**, pp. 4643-4651 (2016).

11. Ohnishi, M., Suzuki, K., and Miura, H. "Effects of uniaxial compressive strain on the electronic-transport properties of zigzag carbon nanotubes", *Nano Research*, **9**, pp. 1267-1275 (2016).

12. Ma, T., Wen, S., Yan, L., Wu, C., Zhang, C., Zhang, M., and Su, Z. "The transport properties of silicon and carbon nanotubes at the atomic scale: a first-principles study", *Phys. Chem. Chem. Phys.*, **18**, pp. 23643-23650 (2016).

13. Reich, S., Maultzsch, J., Thomsen, C., and Ordejon, P. "Tight-binding description of graphene", *Phys. Rev. B*, **66**, pp. 0354121-0354125 (2002).

14. Pakkhesal, M. and Ghayour, R. "Mechanically changed bandgap of single walled carbon nanotube: a third neighbor tight-binding approach", *Cent. Eur. J. Phys.*, **8**, pp. 304-311 (2010).

15. Van Hove, L. "The occurrence of singularities in the elastic frequency distribution of a crystal", *Phys. Rev.*, **89**, p. 1189 (1953).

16. Labany Saha, Amrita Ghosh, Medha Guha, Arpan Deyasi "Analytical computation of band structure and density of states of single-walled carbon nanotube for different structural parameters", *Journal of Electron Devices*, **19**, pp. 1686-1694 (2014).

Biographies

Mehdi Pakkhesal received his MS degree from Shiraz University in Electronics Engineering. He is currently pursuing PhD degree of Electrical Engineering in the Ferdowsi University of Mashhad. He is now working on electronic properties of carbon nanotubes. He has also published several conference and journal papers.

Seyed Ebrahim Hosseini received his BS degree in Electrical Engineering from Isfahan University of Technology, Isfahan, MS degree from Tarbiat Modarres University, Tehran, Iran, and PhD degree in in the same field from Sharif University of Technology, Tehran, Iran in 2001. He is now an Associate Professor of Electronics Engineering at Ferdowsi University of Mashhad. His research areas include nano- and microelectronic devices, SOI transistors, and device modeling and simulation. He has authored or co-authored over than 80 conference and journal papers.